Bridging Classical Optics and Quantum Behavior: Exploration of Quantum Tomography and Bell Test

Yoav Gan,* Shlomi Gelbshtein,† and Sara Gandelman‡
Raymond and Beverly Sackler School of Physics & Astronomy, Faculty of Exact Sciences, Tel Aviv University, Tel Aviv 69978, Israel

Quantum entanglement and state reconstruction are often associated with advanced laboratory infrastructure and single photon sources. In this experiment, we demonstrate that these central ideas of quantum mechanics can be explored using a purely classical optical setup. By analyzing polarization encoded laser pulses with beam splitters, polarizing beam splitters, and half wave plates, we emulate the behavior of a two photon system and recreate the signatures of quantum correlations. Through systematic measurements in multiple polarization bases, we reconstruct the effective density matrix of the simulated state and examine its structure using the tools of quantum state tomography. We further evaluate Bell type correlations using the CHSH inequality, revealing non classical patterns that arise from the controlled polarization correlations of the laser pulses. This experiment provides an accessible hands on platform for engaging with foundational quantum concepts such as tomography, coherence, and Bell inequality tests using classical light.

INTRODUCTION

Quantum mechanics introduced a radically new description of physical systems, one in which the state of a system is not encoded in definite classical properties but in probabilistic amplitudes governed by the wave function. From the early foundational works of von Neumann [1] to the debates surrounding the Einstein-Podolsky-Rosen paradox [2], questions about the nature of measurement, correlations, and physical reality have shaped the modern view of quantum physics. Two of the most powerful frameworks developed to probe these questions are quantum state tomography (QST) and Bell type tests of local realism, both of which allow experimentalists to extract structure that is otherwise hidden within quantum systems. Together, they offer a bridge between operational measurements and the deeper theoretical principles of coherence, entanglement, and nonlocality.

QST provides a systematic way to reconstruct the density matrix of an unknown quantum state from measurable quantities. Although its conceptual motivation comes from early discussions of quantum measurement theory, the practical form of QST emerged later with the pioneering works of Vogel and Risken [3] a, who demonstrated that full quantum states including phase information, coherences, and correlations can be reconstructed directly from experiments. This capability is crucial for studying entanglement, decoherence, and superposition, ** and has made QST indispensable for characterizing photonic entanglement sources [4], quantum gates [5], and high dimensional optical states.**

Bell's inequality emerged from John Bell's landmark 1964 work [6], which showed that certain quantum correlations cannot be explained by any local hidden variable theory. **The experimentally accessible CHSH formulation [7] made it possible to test these ideas directly(is it really true?)**. **Over several decades, increasingly refined experiments closed major loopholes, culminating in the 2015 loophole free demonstrations by **(expand?)**Hensen *et al.* [8], Giustina *et al.* [9], and Shalm *et al.* [10], firmly establishing the nonlocal character of quantum entanglement.**

Recent advances across quantum science have continued to highlight the importance of both QST and Bell type correlation tests. In platforms ranging from photonic entanglement sources to superconducting qubits and trapped ion systems, QST has become a standard tool for characterizing quantum states and verifying entangling operations [4, 11]. Beyond traditional reconstruction techniques, newer approaches, such as machine learning assisted tomography, have enabled the characterization of larger and noisier systems while reducing the number of required measurements [12]. At the same time, Bell type tests remain a powerful method for probing non classical correlations. Modern experiments routinely achieve strong violations of Bell inequalities using high quality entangled photon sources and have demonstrated loophole free tests that underpin device independent quantum communication [8–10]. Together, these developments show how QST and Bell inequalities function not only as foundational probes of quantum mechanics but also as practical tools for validating emerging quantum technologies.

**(more citation - expand on intersting uses and take out the rest)

In our experiment, we bring these ideas into an accessible undergraduate level setup by using classical pulsed laser light to emulate the behavior of entangled photon pairs. Although the source is not inherently quantum, the controlled polarization, beam splitting, and multi basis measurements reproduce the same statistical signatures found in genuine two photon experiments. This allows us to reconstruct density matrices with QST and evaluate the CHSH Bell parameter using ***thresholded intensity measurements***, creating a direct link be-

tween classical optical data and the characteristic markers of quantum entanglement.

Quantum state tomography

In quantum mechanics, the state of a physical system is described by a density matrix ρ, which provides a complete statistical description of the system. generally, for an ensemble of states $\{|\psi_i\rangle\}$ with probabilities p_i, the density matrix defined as

$$\rho = \sum_i p_i \left|\psi_i\right\rangle \left\langle\psi_i\right| . \tag{1}$$

The density matrix contains information about both the populations of different states and the coherences of each state, which encode correlations between components of the quantum state. These coherences are essential for capturing nonclassical phenomena such as superposition and entanglement.

In our system we use a pair of polarization qubits, the natural basis represented by $\{|HH\rangle, |HV\rangle, |VH\rangle, |VV\rangle\}$. Where H stands for Horizontal polarization and V is the vertical ones. The density matrix in this basis is:

$$\rho = \begin{pmatrix} \rho_{HH,HH} & \rho_{HH,HV} & \rho_{HH,VH} & \rho_{HH,VV} \\ \rho_{HV,HH} & \rho_{HV,HV} & \rho_{HV,VH} & \rho_{HV,VV} \\ \rho_{VH,HH} & \rho_{VH,HV} & \rho_{VH,VH} & \rho_{VH,VV} \\ \rho_{VV,HH} & \rho_{VV,HV} & \rho_{VV,VH} & \rho_{VV,VV} \end{pmatrix} . \tag{2}$$

Quantum state tomography (QST) provides a method for experimentally reconstructing ρ by performing measurements in several complementary bases and using the results to infer the matrix elements [3, 13]. For a general two qbit system, these measurements include the H/V basis, the diagonal/anti-diagonal (D/A) basis, and the right/left circular (R/L) basis. which defined as:

$$\begin{aligned} |D\rangle &= \frac{1}{\sqrt{2}}(|H\rangle + |V\rangle), \\ |A\rangle &= \frac{1}{\sqrt{2}}(|H\rangle - |V\rangle), \end{aligned} \tag{3}$$

$$\begin{aligned} |R\rangle &= \frac{1}{\sqrt{2}}(|H\rangle - i\,|V\rangle), \\ |L\rangle &= \frac{1}{\sqrt{2}}(|H\rangle + i\,|V\rangle). \end{aligned} \tag{4}$$

The CHSH test: A practical implementation of Bell's theorem

Bell's theorem [6] provides a way to test whether a system can be described by any local hidden variable model. The CHSH formulation, developed by Clauser, Horne, Shimony, and Holt [7], evaluates four correlation measurements at two angle settings for each party:

$$S = E(a,b) - E(a,b') + E(a',b) + E(a',b'). \tag{5}$$

Local realism imposes the Bell inequality:

$$|S| \leq 2. \tag{6}$$

Quantum mechanics, however, predicts that entangled states can violate this bound and only obey to the bound

$$|S^{(Q)}| \leq 2\sqrt{2}. \tag{7}$$

.

correlation function $E(\alpha,\beta)$ is computed from measured coincidence (or in our case, intensity-thresholded) counts using

$$E(\alpha,\beta) = \frac{N(\alpha,\beta)+N(\alpha_\perp,\beta_\perp)-N(\alpha,\beta_\perp)-N(\alpha_\perp,\beta)}{N(\alpha,\beta)+N(\alpha_\perp,\beta_\perp)+N(\alpha,\beta_\perp)+N(\alpha_\perp,\beta)} \tag{8}$$

where $N(\alpha,\beta)$ is the number of photons measured by both parties, α,β the polarization angles each one measured and $\alpha_\perp \equiv \alpha + 90°$.

EXPERIMENTAL

Experimental Setup

The light source in our setup is a pulsed laser that initially emits vertically polarized pulses. The beam first passes through a neutral density (ND) filter, which attenuates and stabilizes the pulse intensity. After attenuation, the light propagates through a half wave plate (HWP) whose rotation angle determines the output polarization. Because a HWP rotates linear polarization by twice its physical angle, adjusting the plate allows us to prepare the pulse in either the $|V\rangle$ or $|H\rangle$ state. For the purposes of emulating a two level quantum source, the HWP angle is randomly selected for each pulse such that the probability of generating $|V\rangle$ or $|H\rangle$ is 50:50. This randomization mimics a single photon source whose polarization varies from shot to shot, while the underlying optical system remains entirely classical.

After state preparation, the pulse encounters a 50:50 beam splitter (BS), which divides it into two spatial paths corresponding to *Alice* and *Bob*. Each arm contains a polarizing beam splitter (PBS) that separates the incoming pulse according to its polarization, directing horizontal and vertical components into different spatial channels. The outputs of the PBS are imaged onto two consumer-grade cameras (Logitech C270) per arm, which record the intensity of each pulse. By integrating the pixel values over a selected region of interest (ROI), we obtain a quantitative measure of the intensity in each polarization channel, enabling us to reconstruct polarization statistics and perform quantum state tomography measurements. A schematic of the full optical layout is shown in Fig. 1.

Derivation of analogous entanglement with pulsed source

In this section, we model our classical experimental setup as an effective quantum system. We establish the theoretical framework necessary to define entanglement within this context, enabling the investigation of Bell's inequality violations. Finally, we predict the density matrix constructed by the tomography allowing an experiment benchmark to verify the theory.

Quantum state tomography(ψ_1)

source preparation

The pulsed laser emits coherent light pulses that travels trough a HWP that change the polarization randomly from $|V\rangle$ to $|H\rangle$ hence we got:

$$p(|V\rangle) = p(|H\rangle) = \frac{1}{2}. \tag{9}$$

Where $P(I)$ the probability for each state $I \in \{|H\rangle, |V\rangle\}$

Beam splitter transformation

When a pulse prepared in the polarization state $\left|P^{(i)}\right\rangle$, with $P^{(i)} \in \{|V\rangle, |H\rangle\}$, reaches the 50:50 beam splitter, it is divided into two identical outgoing modes. The transformation can be written as

$$\left|P^{(i)}\right\rangle \longrightarrow \left|P_A^{(i)}\right\rangle \otimes \left|P_B^{(i)}\right\rangle, \tag{10}$$

where $\left|P_A^{(i)}\right\rangle$ and $\left|P_B^{(i)}\right\rangle$ represent the coherent states propagating toward Alice and Bob, respectively with the probabilities

$$P(P_A, P_B) = \begin{cases} \frac{1}{2}, & \text{if } (P_A, P_B) = (H_A, H_B) \text{ or } (V_A, V_B), \\ 0, & \text{otherwise.} \end{cases} \tag{11}$$

Therefor we get the state of the system:

$$|\psi_1\rangle = \frac{1}{\sqrt{2}} \left(|H_A, H_B\rangle + |V_A, V_B\rangle\right), \tag{12}$$

modified experiment setup

Now we add a HWP with $\lambda/2 = 45°$ to Bob path so the polarization of Bob Light changes

$$|V\rangle \leftrightarrow |H\rangle$$

while Alice's polarization remain identical to the source. Again the source sends randomize polarization with equal probabilities. so now we get

$$\left|P^{(i)}\right\rangle \rightarrow \begin{cases} |V_A\rangle \otimes |H_B\rangle & \text{if } P = V \\ |H_A\rangle \otimes |V_B\rangle & \text{if } P = H \end{cases} \tag{13}$$

Therefor the system's state is now

$$|\psi_2\rangle = \frac{1}{\sqrt{2}} \left(|H_A, V_B\rangle + |H_A, V_B\rangle\right), \tag{14}$$

Reconstructed density matrix

For the tomography we will remind the assumption that we are in a pure system meaning there is only one state sent in each of the system states. In this case we get $\rho_{ii} = P(i), \rho_{ij} = \sqrt{P(i)P(j)}$ where i in the second phrase is the component of the system vector in the base $\{|HH\rangle, |HV\rangle, |VH\rangle, |VV\rangle\}$. Hence we conclude for the first state:

$$\rho_{\text{recon}} = \begin{pmatrix} 0.5 & 0 & 0 & 0.5 \\ 0 & 0 & 0 & 0 \\ 0 & 0 & 0 & 0 \\ 0.5 & 0 & 0 & 0.5 \end{pmatrix}. \tag{15}$$

Which matches the density matrix

$$\rho_{\psi_1} = |\psi_1\rangle \langle\psi_1| \tag{16}$$

and for the second state

$$\rho_{\text{recon}} = \begin{pmatrix} 0 & 0 & 0 & 0 \\ 0 & 0.5 & 0.5 & 0 \\ 0 & 0.5 & 0.5 & 0 \\ 0 & 0 & 0 & 0 \end{pmatrix}. \tag{17}$$

Which matches the density matrix $\rho_{\psi_2} = |\psi_2\rangle \langle\psi_2|$

Quantum state tomography measurements

In this part of the experiment we aim to measure two distinct polarization configurations, corresponding to the states described in Eqs. (12) and (14).

Equation (12) defines the state $|\psi_1\rangle$, in which the polarizations detected by Alice and Bob are *correlated*. In this case, if the source emits a pulse polarized in the $|H\rangle$ state, both detectors record the same polarization outcome. Similarly, $|V\rangle$-polarized pulses are jointly detected as $|V\rangle$ by both arms.

$$|\psi_1\rangle = \frac{1}{\sqrt{2}} \left(|H_{Alice}, H_{Bob}\rangle + |V_{Alice}, V_{Bob}\rangle\right) \tag{18}$$

Equation (14) specifies the state $|\psi_2\rangle$, where Alice and Bob measure *anti-correlated* outcomes. Here Alice

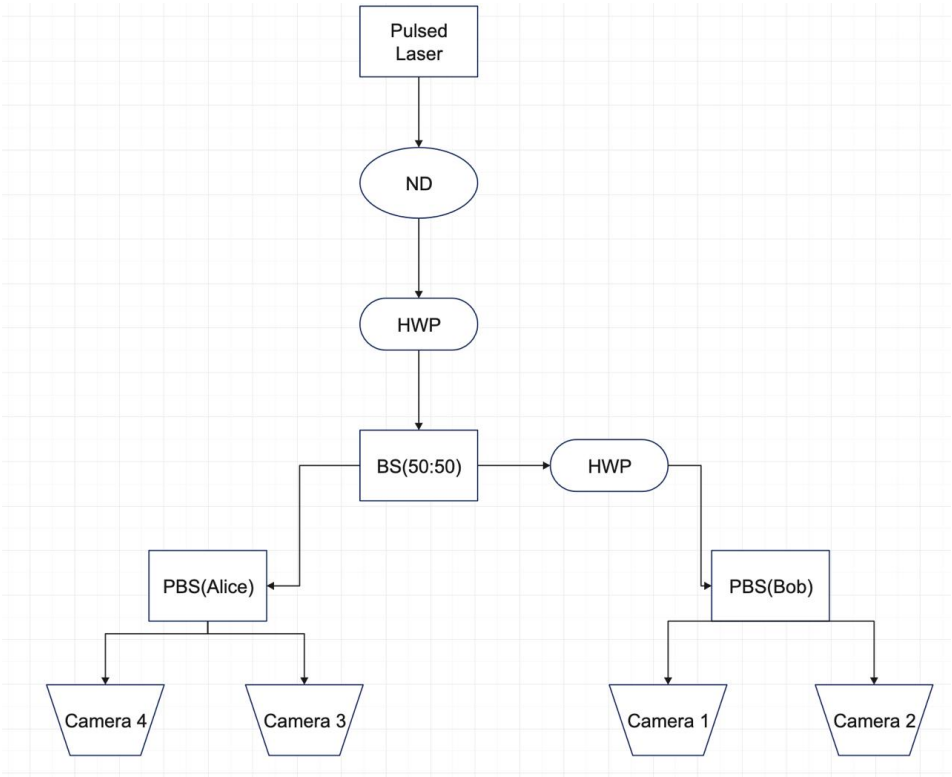

FIG. 1: Experimental setup simulating single-photon behavior using classical light. A randomly polarized light beam is divided by a 50:50 Beam Splitter (BS) into two identical spatial modes. At each receiving station, a Polarizing Beam Splitter (PBS) separates the polarization directing them to distinct detectors. A Half-Wave Plate (HWP) placed in Bob's arm enabling the measurement of various polarization correlations. Abbreviations: BS - beam splitter; PBS - polarizing beam splitter, HWP - half wave plate.

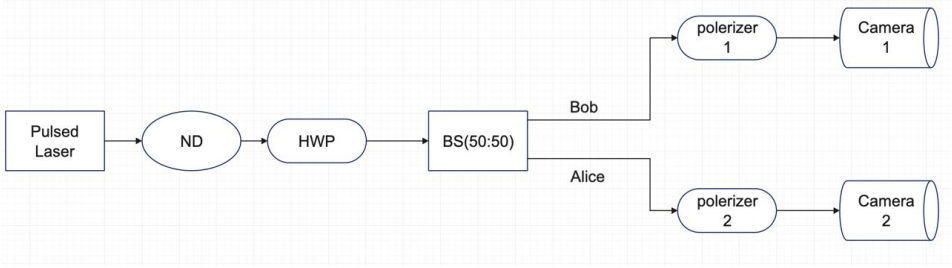

FIG. 2: sketch of the system used to perform bell test via classical setup. The setup consist of a random polerized lazer, a ND to adjust the light intensity and Alice and Bob, each with a polerizer at angle α and β respectively. The system measure bell's parameter by measuring Alice and Bob outcom in series of different α, β angles

records the original polarization sent by the source, while Bob measures the orthogonal polarization. This configuration is implemented experimentally by rotating the half-wave plate (HWP) placed in front of Bob's detection arm by 45° relative to the optical axis.

$$|\psi_2\rangle = \frac{1}{\sqrt{2}} \left(|V_{Alice}, H_{Bob}\rangle + |H_{Alice}, V_{Bob}\rangle \right) \tag{19}$$

To realize both states $|\psi_1\rangle$ and $|\psi_2\rangle$, we randomize the polarization of each emitted pulse. This randomness ensures that the ensemble of pulses effectively behaves as a mixed input state, allowing us to emulate the superposition like correlations expected from a two photon entangled system. The resulting correlations constitute the necessary dataset for performing quantum state tomography and for evaluating Bell type inequalities.

Pulse detection is carried out using camera based photodetectors operating at a frame rate of 30 fps. The recorded video is processed using MATLAB, where each pulse is identified and integrated over a predefined region of interest (ROI) corresponding to the beam location.

For every frame, we compute the total intensity within each ROI. To extract discrete detection events, we apply a threshold to the intensity traces of each camera. This suppresses background noise and yields a binary (1/0) record indicating whether a valid pulse has been detected. These binary outcomes form the measurement data used for reconstructing the density matrices.

Bells inequality measurements

Bell's parameter S provides a quantitative measure of whether the correlations observed between two subsystems can be described by any local realistic theory. In quantum mechanics, entangled states can violate the classical CHSH bound $|S| \leq 2$, demonstrating the presence of nonlocal correlations that cannot be reproduced by classical physics. Measuring S in our experiment therefore enables a direct comparison between the correlations produced in our optical setup and those expected from genuinely entangled photon pairs.

To evaluate the Bell parameter S as defined in Eq. (5), we modify the detection stage by removing the PBSs in front of Alice and Bob and replacing them with linear polarizers. Each polarizer transmits only a single polarization component, so only one camera is required on each arm of the interferometer. The measurement settings are defined by the polarizer angles: Alice's angle is denoted by α and Bob's by β, as illustrated in Fig. 2. With this configuration, the correlation between Alice's and Bob's detection outcomes can be directly measured as a function of the chosen analysis angles.

To determine the coincidence like quantity $N(\alpha, \beta)$ appearing in Eq. (8), we record the intensities registered by both cameras for a series of polarizer settings (α, β). The cameras capture the pulsed signal at a frame rate of 30 fps. The resulting video footage is processed in MATLAB following the same procedure as in the QST analysis: for each detection channel we define a region of interest (ROI) and extract the integrated pulse intensity from each frame. A threshold is then applied to discriminate valid pulses from background noise, effectively mapping each detection event onto a binary outcome (0 or 1). Crossing the threshold corresponds to detecting a pulse whose polarization is aligned with the chosen polarizer basis. These binary outcomes are then used to compute the required correlations $E(\alpha, \beta)$ and ultimately determine the Bell parameter S.

RESULTS

Quantum tomography

The results shows a successful reconstruction of the sent states density matrices. For the initial configuration ψ_1 (link to photos), the Quantum State Tomography (QST) results demonstrate excellent agreement with theoretical predictions. We observed perfect correlations between Alice's and Bob's measurements, they both measured the same state each time. the reconstructed density matrix 3 (a-c) is consistent with the theoretical density matrix given in Eq. (15), which corresponds to the state defined in Eq. (12). The minor deviations observed in the 50-bit sample can be attributed to the limited sample size, since change in a few samples result in significant percentage discrepancies.

In the second phase(link to photos), the Half-Wave Plate (HWP) was rotated to a configuration where Alice and Bob measure opposite polarization states. As expected, strong anti-correlations were observed - Each time Bob detect (V) Alice detected (H), and vice versa. The obtained density matrix shows high fidelity with the theoretical density matrix described in Eq. (17), corresponding to the state in Eq. (14).

Collectively, these results confirm that the experimental setup accurately reconstruct the target states, thereby validating its capability to measure quantum effects and, specifically, to test the violation of Bell's inequality.

Bell's test

Using the CHSH test, we calculated the Bell parameter S to quantify the correlations between Alice's and Bob's measurements. The polarization states were measured at angles α and β, respectively, as detailed in Table **??**, and coincidence counts were recorded. To isolate the signal from background noise, a discrimination threshold was applied to the detector pulses.

A significant asymmetry was observed in the detection rates; Alice's measured intensity was approximately an order of magnitude higher than Bob's. This discrepancy is likely attributable to instrumental imperfections, such as differing efficiencies in the cameras or the Polarizing Beam Splitters (PBS). Consequently, independent thresholds were calibrated for each detection channel.

Post-measurement analysis yielded a Bell parameter of $S = 2.30$. This violation of the classical bound ($|S| \leq 2$) indicates that local hidden variable theories cannot account for the observed correlations, consistent with quantum mechanical predictions.

It is worth noting that the measurement at $\alpha = 90°, \beta = 112.5°$ yielded a significantly lower light intensity compared to the other settings. However, this anomaly does not effect the final Bell parameter S since

TABLE I: Measured values of $N(\alpha, \beta)$ for different polarizers settings.

α	β	N	α	β	N
$-45°$	$-22.5°$	12	$45°$	$-22.5°$	8
$-45°$	$22.5°$	7	$45°$	$22.5°$	5
$-45°$	$67.5°$	4	$45°$	$67.5°$	9
$-45°$	$112.5°$	12	$45°$	$112.5°$	9
$0°$	$-22.5°$	13	$90°$	$-22.5°$	0
$0°$	$22.5°$	11	$90°$	$22.5°$	0
$0°$	$67.5°$	0	$90°$	$67.5°$	10
$0°$	$112.5°$	0	$90°$	$112.5°$	0

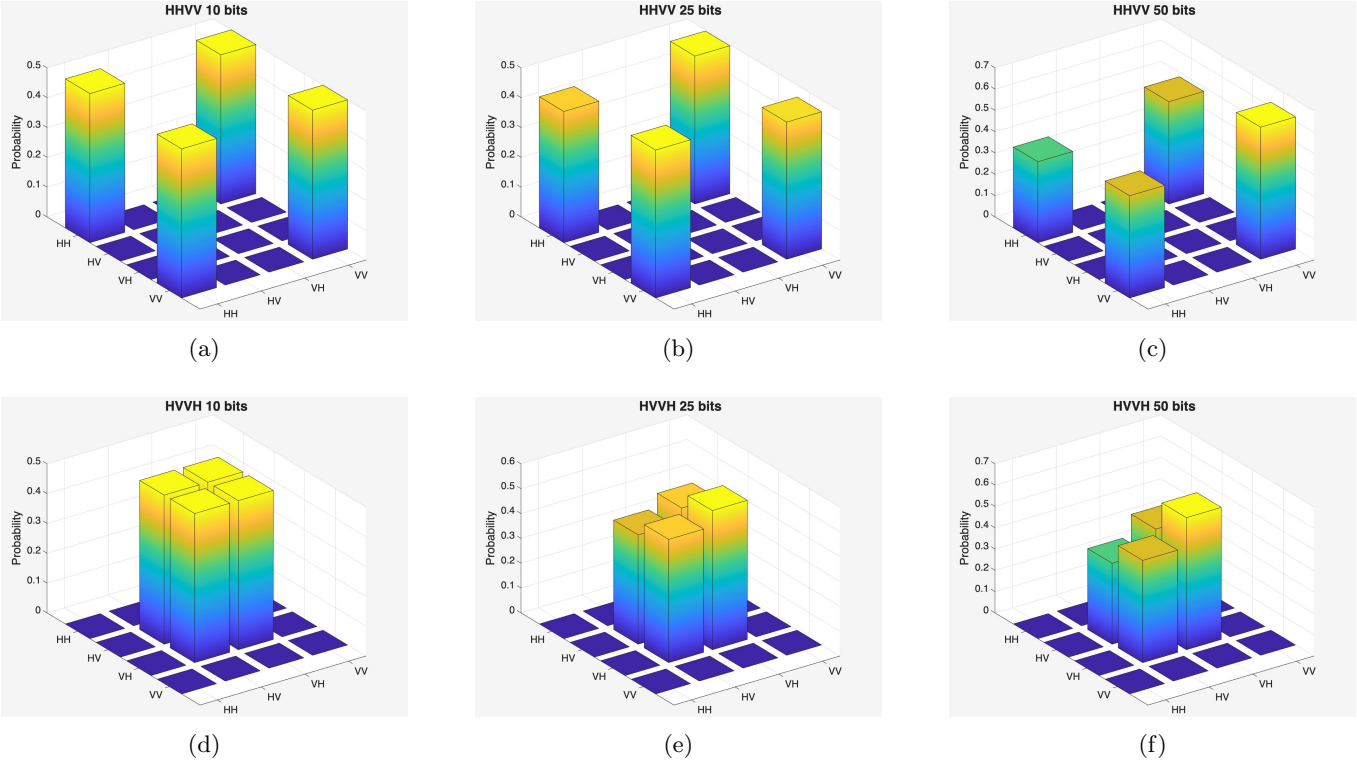

(a) (b) (c)

(d) (e) (f)

FIG. 3: The results are presented as 3D bar graphs representing the density matrix for sample sizes of 10, 25, and 50 bits. The aligned configuration (a)–(c), where Alice and Bob measure identical polarizations, consistent with the state described in Eq. 14 .The orthogonal configuration (d)–(f), achieved by rotating Bob's Half-Wave Plate (HWP), resulting in the correlations described in Eq. 12. Column heights represent the magnitude of the matrix elements. The accuracy of the reconstructed density matrix across varying data lengths demonstrates the reliability of the experimental setup in emulating super position state and capturing polarization corelation

his measurement enters only into the calculation of the $E(0°, 22.5°)$ term. In our data, the terms subtracted in the numerator were zero so the numerator and denominator became identical, yielding a correlation value of $E = 1$.

DISCUSSION

Our results demonstrate that the classical optical setup is capable of reliably emulating key signatures of quantum behavior. The reconstructed density matrices match the expected structures for the two simulated states, and the measured Bell parameter of $S = 2.3$ exceeds the classical bound of $|S| \leq 2$. Together, these findings indicate that the system reproduces the polarization correlations

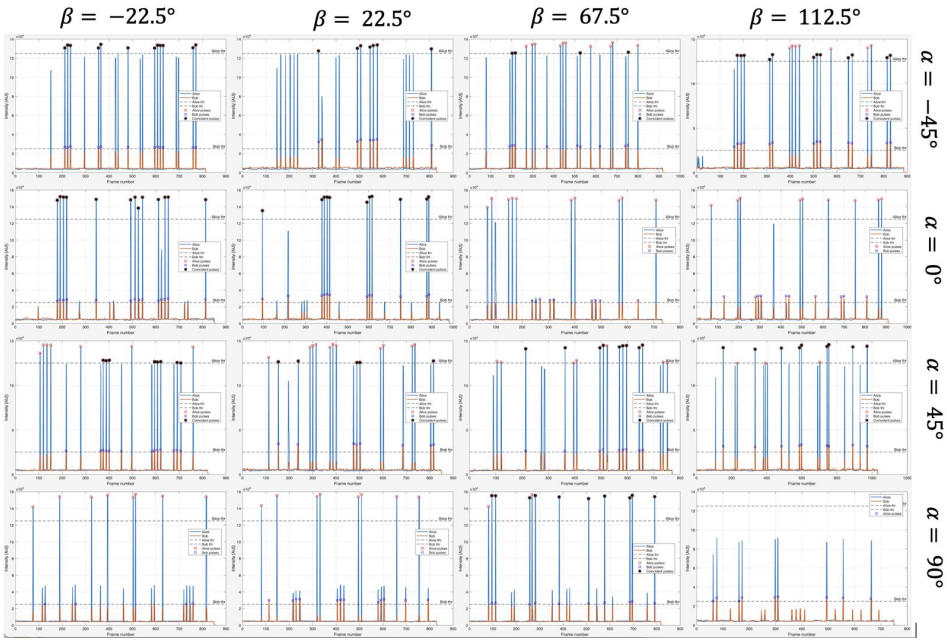

FIG. 4: measured light intensity over time for all the different angles α, β. A threshold filter is applied to exclude noise and to count only the relevant picks. Note, that there are two threshold filters one for each party. We used those measures to calculate Bells parameter S and to get the experimental value $S = 2.30$ which is higher than the classical bound $|S| \leq 2$

characteristic of entangled photon experiments with good accuracy.

Tomography accuracy and setup reliability

The quantum state tomography results, together with the reconstructed density matrices, show a clear correspondence between the measured probabilities and the theoretical expectations for both ψ_1 and ψ_2, consistent with established QST procedures [14]. This agreement indicates that the experimental setup was properly aligned and that the key optical components such as the half wave plates and polarizing beam splitters operated as intended. Although minor alignment imperfections can influence the measurements, their impact appears limited. Notably, the density matrices obtained for the 50 bit datasets are slightly less accurate than those from lower bit counts, contrary to the theoretical expectation that larger samples improve reconstruction. This deviation is likely due to the relatively small sample sizes, where changes in only a few detection events can produce large percentage shifts. Even so, the setup demonstrates reliable state reconstruction, and larger statistical samples would further enhance accuracy. Overall, the system provides a robust educational platform that allows undergraduate students to explore quantum correlations and perform meaningful QST measurements.

Bell's inequality violation

The measured Bell parameter of $S = 2.30$ indicates that the correlations between Alice and Bob clearly exceed the classical CHSH bound of $|S| \leq 2$, consistent with the observation that certain classical optical fields can reproduce quantum like correlation structures [15]. Such a value reflects correlation patterns characteristic of quantum systems, despite the fact that our setup is entirely classical. This result therefore supports the effectiveness of our apparatus in emulating key features of quantum entanglement and reproducing the non-classical statistics associated with it. The deviation from the quantum maximum of $2\sqrt{2}$ can be attributed to limitations inherent to the classical optical implementation such as imperfect polarization control, detector noise, and the absence of true single photon behavior, which naturally reduce the achievable correlation strength while still allowing a clear violation of the classical bound.

Emulating Quantum Phenomena with Classical Optics

As demonstrated by the reconstructed density matrices and the measured value of the Bell parameter, the classical optical setup succeeds in emulating key features of a genuinely quantum system. Despite relying entirely on classical light, the experiment reproduces the sta-

tistical structures associated with the states $|\psi_1\rangle$ and $|\psi_2\rangle$, enabling meaningful exploration of superposition-like correlations and entanglement analogues, consistent with known examples of non separable structures in classical optics [16]. This makes the setup particularly valuable in an undergraduate environment: students can perform hands-on measurements that mirror quantum optical experiments without the cost, fragility, or complexity of true single-photon sources. Moreover, by engaging directly with reconstructed states and Bell-type correlations, students gain practical exposure to foundational concepts such as coherence, nonlocal correlations, realism, and locality that are often discussed only abstractly in coursework. With improved optical components and larger data sets, the same classical framework could further approximate ideal quantum behavior, allowing deeper investigation of quantum information phenomena while remaining accessible and inexpensive. As a whole, the setup demonstrates that even a fully classical apparatus can serve as an effective gateway to hands-on exploration of quantum correlations and the principles underlying modern quantum science.

CREDITS

* yoavgan@mail.tau.ac.il
† shlomig@mail.tau.ac.il
‡ sarag@mail.tau.ac.il

[1] J. von Neumann, *Mathematische Grundlagen der Quantenmechanik* (Springer, Berlin, 1932).
[2] A. Einstein, B. Podolsky, and N. Rosen, Physical Review **47**, 777 (1935).
[3] K. Vogel and H. Risken, Physical Review A **40**, 2847 (1989).
[4] P. G. Kwiat, K. Mattle, H. Weinfurter, A. Zeilinger, A. V. Sergienko, and Y. Shih, Physical Review Letters **75**, 4337 (1995).
[5] I. L. Chuang and M. A. Nielsen, Journal of Modern Optics **44**, 2455 (1997).
[6] J. S. Bell, Physics **1**, 195 (1964).
[7] J. F. Clauser, M. A. Horne, A. Shimony, and R. A. Holt, Physical Review Letters **23**, 880 (1969).
[8] B. Hensen *et al.*, Nature **526**, 682 (2015).
[9] M. Giustina *et al.*, Physical Review Letters **115**, 250401 (2015).
[10] L. K. Shalm *et al.*, Physical Review Letters **115**, 250402 (2015).
[11] I. L. Chuang, N. Gershenfeld, and M. G. Kubinec, Proceedings of the National Academy of Sciences **94**, 14912 (1997).
[12] G. Torlai, G. Mazzola, J. Carrasquilla, M. Troyer, R. G. Melko, and G. Carleo, Nature Physics **14**, 447 (2018).
[13] D. T. Smithey, M. Beck, M. G. Raymer, and A. Faridani, Physical Review Letters **70**, 1244 (1993).
[14] D. F. V. James, P. G. Kwiat, W. J. Munro, and A. G. White, Physical Review A **64**, 052312 (2001).
[15] R. J. C. Spreeuw, Foundations of Physics **28**, 361 (1998).
[16] A. Aiello, P. Banzer, M. Neugebauer, and G. Leuchs, Nature Photonics **9**, 789 (2015).